POLISH MARITIME RESEARCH Special Issue 2018 S1 (97) 2018 Vol. 25; pp. 85-93
10.2478/pomr-2018-0028

NUMERICAL SIMULATION OF CUSHIONING PROBLEM FOR BLUNT BODIES USING BOUNDARY ELEMENT METHOD

Mojtaba Barjasteh
Hamid Zeraatgar
Amirkabir University of Technology, Tehran, Iran

ABSTRACT

Induced air pressure and resulting free surface profile due to air cushioning layer is studied. The study is mainly focused on 2D blunt circular bodies with constant downward speed. The problem is first solved for the air flow between the body and the free surface of the water. Then the results are employed to solve the problem for the water problem, numerically. Both air and water problem are assumed to be governed by Laplace potential equation. Depending on the induced pressure and velocity of the escaping air flow from cushioning layer, compressibility of the air is also included in the modeling. Gravitational acceleration is also included in the model. An iterative boundary element method is used for numerical solution of both air and water problems. Instantaneous pressure distribution and free surface profile are evaluated for different bodies. The results of calculation for large blunt bodies show that inviscid potential method can fairly approximate the problem for large blunt bodies. Additionally, the behavior of the air pressure for the very blunt body is impulsive and the magnitude of the peak pressure is in order of impact pressure of water entry. The obtained results are compared with analytical method. The comparison shows that as the bluntness of a body increases, the better agreement is concluded.

Keywords: Air cushion, compressible potential flow, water entry, slamming

INTRODUCTION

Hydrodynamic evaluation of several typesof marine vehicles are based onsolution of water entry problem. It is common to study a 3D geometry of a vessel by 2D sections along ship length. A 2D section of a ship is a classical water entry problem. The water entry problem may be solved analytically, numerically as well as by experiment. The water entry problem is correlated to some other phenomena which complicates the evaluation of the problem. One of these phenomena is the cushioning layer right before impact. As a body drops and get close to free surface of the water, air between body and the water surface may not scape and compressed as body closes to the surface. An air layer is formed between the body and free surface of the water. Based on the mass continuity, the velocity of escaping air flow from the layer exponentially increases as the body closes the surface. Since the gap layer is usually very narrow and the body momentum is generally high, the induced air pressure along the cushioning layeris very high. Physically, for the force balancein vertical direction, the free surface is deformed to balance the induced air pressure at the air-water interface. This deformation causes a multipoint impact rather than asingle point impact as it is assumed in most of water entry theories. Depending on the shape of impacting body and deformed free surface profile, some volume of air may be entrapped during entry. The cushioning layer reduces the impact speed as well as the hydrodynamic impact pressure

due to air drag and compression of entrapped air, respectively. Thus accurate prediction of maximum impact pressure requires considering the cushioning layer particularly for high speed impact of blunt bodies.

There are several researches on the topic mainly focused on the evaluation of impact pressure and free surface deformation in bubble dynamics and droplet impacts. The survey was started by Verhagen[1] who modeled the air layer using a channel flow problem with constant geometry of moving walls. He concluded that the lubrication equation[2] may properly simulate the channel flow instead of traditional equations. The proposed model was just a case study and cannot be further developed for different geometries. The next significant try was made by Asryan[3]. He recommended two different formulation including inviscid incompressible and viscous compressible. Both models are available for initial stage of the body motion when the surface deformation isnegligible. Thus, the free surface deformation was not investigated. The obtained results overestimate the pressure and underestimate the air speed particularly at throat of the air gap layer. Wilson [4] suggested a non-dimensional asymptotic model to simulate the problem based on two dimensional Navier-Stokes equation. The model is initially stable but as the body gets closer to the free surface the results are unstable. This instability also occurred for blunter bodies. Hicks and Purvis [5] conducted a great series of experiments and analytical research on the problem. They studied the problem in all details primarily for a bubble impact onto liquid or solids and its resulting deformation due to presence of cushioning layer. Different parameters such as viscosity dissipation, compressibility, topography and the validity of the proposed models are fully discussed in their works. They employed different forms of lubrication equation for the air problem and potential flow for the bubble deformation. They validated the obtained results with some experimental research [8] and with different available theories.

All studies show that the dimensional analysis generally controls the problem and its corresponding governing equation. Different research were also made on this analysis to provide some better understanding of the problem such as those carried out by Mandre and Brenner [9] and Smith et. all[10]. They introduced different time and length scales based on the different configuration of the problem. On that basis, they concluded which governing equations such as lubrication equation, incompressible potential flow and compressible flow are applicable. Some experimental studies also investigated different applications of cushioning problem. Two distinctive experimental researches are those carried out by Marston et. all[11] and Tran et. all[12]. Both studies were concentrated on cushioning layer and the resulting air entrapment for small bodies. Some unique visualization and precise measurement were reported. One of the interesting tests results is to determine a scaling law for non-dimensional volume of air entrapment. This scaling simply implies that the volume of air entrapment depends to the Stokes number of the flow. This relation is changed for different regimes of the flows. There are also several research to investigate the problem such as those conducted by Lewison and Maclean [13], Thoroddsen et. all[14] and Bouwhuis et. all[15] which have different contribution to the problem consideration.

This study, as a relatively simple approach, represents a fully potential flow for both air and water problem and disregards the lubrication equation for very narrow air layer. Therefore the validity of the formulation is limited to high speed impact of blunt bodies. A fast and practical boundary element method is employed to evaluate all desired parameters of the problem. The proposed method can be efficiently used for developing a commercial software in full prediction of water impact including air cushioning effects.

FORMULATION

The present model investigates the cushioning problem in water entry of blunt body such as depicted in Figure 1. A blunt body with downward speed of v_0 moves toward to the water free surface which is initially at the rest. The downward speed is assumed to be constant and vertical, for the sake of simplicity. Since the body is essentially blunt and its speed is assumed to be high enough, the dominant phenomenonforfree surface deformation is normal pressure balance. Therefore the viscosity is neglected for both air and water problem. Two length scales are defined here to check the model validity as depicted in Figure 1. The first one in horizontal direction and shows the maximum length of disturbed free surface which is called *L*. The second length scale indicates the maximum depth of free surface, *H,* due to air pressure. The present formulation is not valid when *H<<L*. It may be shown that when *H<<L,* the viscous terms cannot be neglected anymore.

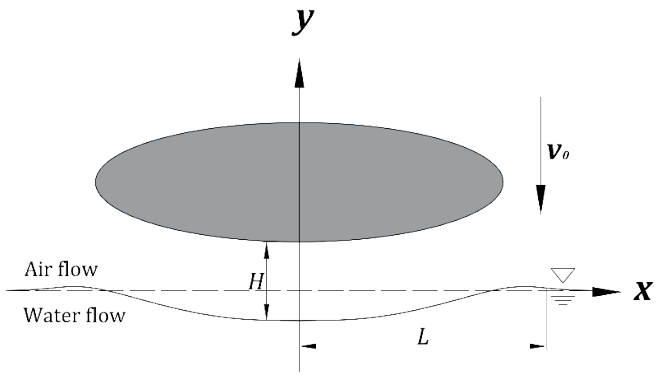

Fig. 1. Problem definition, the free surface profile is schematic and exaggerated

According to the problem configuration, both flows are assumed to be potential. The water flow remains always incompressible. Thus the governing equation in the water flow is the Laplace equation.

$$\frac{\partial^2 \phi}{\partial x^2} + \frac{\partial^2 \phi}{\partial y^2} = 0 \qquad (1)$$

The governing equation for the air flow is also the Laplace equation, since it is incompressible. However, as the body is very close to the free surface, high pressure may be induced to the air layer and the escaping speed of air flow considerably increases as a result. At this condition, the air compressibility should be taken into account. From Euler equation in term of differentials, the pressure and momentum correlated to each other.

$$dP = -\rho V dV \tag{2}$$

Where V is the total velocity. This equation is independent to the flow directions for the problem under consideration. Thus, the velocity components can be evaluated from potential equations.

$$dP = -\frac{\rho}{2}\left[\left(\frac{\partial^2\phi}{\partial x^2}\right)^2 + \left(\frac{\partial^2\phi}{\partial y^2}\right)^2\right] \tag{3}$$

The flow is assumed to be isentropic and the air fluid is an ideal gas. So, the pressure gradient is a function of density gradient.

$$\left(\frac{dP}{d\rho}\right)_s = c^2 \tag{4}$$

where c is the local speed of the sound in the air flow. Substituting the pressure gradient with density gradient results in:

$$d\rho = -\frac{\rho}{2c^2} d\left[\left(\frac{\partial^2\phi}{\partial x^2}\right)^2 + \left(\frac{\partial^2\phi}{\partial y^2}\right)^2\right] \tag{5}$$

Continuity equation is also always valid for both compressible and incompressible flow. Substituting the velocity potential in continuity equation yields:

$$\rho\left(\frac{\partial^2\phi}{\partial x^2} + \frac{\partial^2\phi}{\partial y^2}\right) + \frac{\partial\phi}{\partial x}\frac{\partial\rho}{\partial x} + \frac{\partial\phi}{\partial y}\frac{\partial\rho}{\partial y} = 0 \tag{6}$$

Removing density differential from Euler and continuity equation results in the final governing equation of compressible potential flow:

$$\left[1 - \frac{1}{c^2}\left(\frac{\partial\phi}{\partial x}\right)^2\right]\frac{\partial^2\phi}{\partial x^2} + \left[1 - \frac{1}{c^2}\left(\frac{\partial\phi}{\partial y}\right)^2\right]\frac{\partial^2\phi}{\partial y^2} - \frac{2}{c^2}\left(\frac{\partial\phi}{\partial x}\right)\left(\frac{\partial\phi}{\partial y}\right)\frac{\partial^2\phi}{\partial x\partial y} = 0 \tag{7}$$

and

$$c^2 = c_0^2 - \frac{k-1}{2}\left[\left(\frac{\partial\phi}{\partial x}\right)^2 + \left(\frac{\partial\phi}{\partial y}\right)^2\right] \tag{8}$$

where c_0 and k are stagnation local speed of sound and ratio of air specific heat, respectively. The derived governing equation is nonlinear partial differential equation with only one unknown parameter in term of flow potential. This equation can be solved numerically. However, due to moving free surface profile, the solution is not easy. To overcome this drawback, the nonlinear PDE is linearized. One can employ a perturbation analysis for linearization of the problem. The perturbation velocity potential can be defined as $\hat{\phi} = \phi_t - \phi_u$ where ϕ_t and ϕ_u are total and uniform velocity potential. Perturbation velocity components can also be evaluated similarly as $u = u_\infty + \hat{u}$ and $v = v_\infty + \hat{v}$. For vertical downward speed of the body the uniform velocity is the body velocity. To substitute the perturbation parameters in the governing equation, local speed of sound should be stated as a function of perturbation velocity components. Such a task is carried out employing stagnation form of energy equation:

$$\frac{c_\infty^2}{k-1} + \frac{v_0^2}{2} = \frac{c^2}{k-1} + \frac{(\hat{u})^2 + (v_0 + \hat{v})^2}{2} \tag{9}$$

Mach number of uniform flow is very small in comparison with the perturbation velocity components. Substituting the local speed of sound from energy equation into the governing equation yields.

$$\frac{\partial^2\hat{\phi}}{\partial x^2} + (1 - M_\infty^2)\frac{\partial^2\hat{\phi}}{\partial y^2} = 0 \tag{10}$$

The derived equation is a linear partial differential equation but in terms of perturbation potentials. This equation can be transformed from physical domain to a computational domain byintroducing new variables.

$$\begin{aligned} \psi &= x \\ \xi &= (1 - M_\infty^2)^{-\frac{1}{2}} y \end{aligned} \tag{11}$$

This transformation just changes the horizontal coordinate system and does not change the behavior of the equation. Using chain rule of differentiation, one can find new differentials:

$$\begin{aligned} \frac{\partial^2\hat{\phi}}{\partial x^2} &= \frac{\partial^2\hat{\phi}}{\partial\psi^2} \\ \frac{\partial^2\hat{\phi}}{\partial y^2} &= \frac{1}{1 - M_\infty^2}\frac{\partial^2\phi}{\partial\xi^2} \end{aligned} \tag{12}$$

Recalling the new parameters into the governing equation yields:

$$\frac{\partial^2\hat{\phi}}{\partial\psi^2} + \frac{\partial^2\hat{\phi}}{\partial\xi^2} = 0 \tag{13}$$

This is a new form of Laplace equation for transformed perturbation velocity. Now, the air flow problem is always governed by Laplace equation for incompressible potential

flow, Equation 1, and another one for compressible potential flow in transformed computational domain, Equation 13. This boundary value problem can be solved if boundary condition at all boundaries are known. Since the geometry of the problem is symmetric, the solution of the problem is carried out for a half space. The boundary condition on the body is no flux boundary condition.

$$\frac{\partial \phi}{\partial n} = V.n \tag{14}$$

where n is the normal vector pointing outward the body surface. On the free surface, both kinetic and kinematic free surface boundary condition should be satisfied.

$$v = \frac{D\eta}{Dt} = \left[\frac{\partial \eta}{\partial t} + u\frac{\partial \eta}{\partial x}\right] \tag{15}$$

$$\frac{\partial \phi}{\partial t} + \frac{1}{2}|\nabla \phi|^2 = g\eta - \frac{\sigma}{\rho_w}\left[\frac{|\partial^2 \eta/\partial x^2|}{(1+(\partial \eta/\partial x)^2)^{3/2}}\right] - \frac{P_a}{\rho_w} \tag{16}$$

here σ, η, P_a and ρ_w are air-water surface tension, free surface profile, air pressure on the interface and water density, respectively. The potential vanishes for far field condition.

$$\phi(\infty, 0) = 0 \tag{17}$$

The free surface profile is assumed to be at rest as an initial condition or $\eta(x, 0) = 0$. Similar boundary conditions can be also derived for the water problem and a transformed form of compressible potential flow. The boundary condition on the water bed can be a wall or a far field condition. It can be shown for a deep water problem,both boundary conditions result in the same potentials. Although the water is deep enough, the problem can be also solved for a shallow water by adjusting the height of symmetry line. At this condition the water bed boundary condition can only be wall boundary condition not a far-field one.

NUMERICAL IMPLEMENTATION:

Depending on the problem configuration and the computational regions, the problem is governed by three different governing equation including an incompressible potential equation for air flow, an incompressible potential equation for water problem and finally a compressible potential flow for high speed escaping air flow. All of the governing equations are in general form of Laplace equation. The most common and practical method of solving such an equation is to employ boundary element method. The numerical solution is started by incompressible potential air flow. First the boundaries of the problem are discretized into linear elements. The important boundaries are Γ1, Γ2 and Γ3 indicating the body, the symmetry line and the free surface. There is also a fourth boundary that closes the problem domain to the farfield boundary condition.

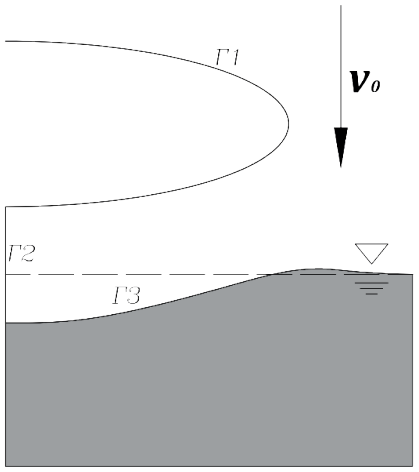

Fig. 2. Computational domain and the main boundaries

The elements are constant and linear. So there is one integration point on the middle of each element called the point q. It can be readily shown that for any in-domain arbitrary point such as P, the potential can be related to distributed sources on each element using second identity of Green'sTheoremin form of an integral equation.

$$\phi(P) = -\int_\Gamma \left[\lambda(F,q)\frac{\partial \phi(q)}{\partial n_q} - \phi(q)\frac{\partial \lambda(F,q)}{\partial n_q}\right] ds_q \tag{18}$$

where λ is the fundamental solution of Laplace equation for two-dimensional problem.

$$\lambda = \frac{1}{2\pi}\ln r\,(F,q)$$
$$\frac{\partial \lambda}{\partial n_q} = \frac{1}{2\pi}\frac{\cos\left(\angle(r,n)\right)}{r} \tag{19}$$

and $r = |q - F|$ is the distance vector. The integral equation can be represented in summation of influence coefficients $\hat{H}$ and $\hat{G}$ assuming constant distribution of potential on each element [16].

$$-\frac{1}{2}\phi^i + \sum_{j=1}^{N}\hat{H}_{ij}\phi^j = \sum_{j=1}^{N}\hat{G}_{ij}\frac{\partial \phi^j}{\partial n} \tag{20}$$

where N is the total number of elements. The influence coefficients are only functions of the problem geometry and they are known. The problem is a mixed Dirichlet-Neumann boundary condition. The number of known and unknown parameters are the same and the problem changes to a system of algebraic equations. So, a linear system of algebraic equations can be rearranged to find unknowns. The numerical solution starts similar to all linear constant boundary element

method. At the first time step the initial position of the body and its downward velocity are known. Additionally, the initial free surface profile is at the rest. The solution of the problem at the first time step results in a potential fields in the air flow. Furthermore, the potentials on the free surface are also evaluated. For updating the free surface profile, it is needed to have the data of the next time step. At the first time step the free surface is assumed to be a wall boundary condition, for the sake of simplicity. This assumption is only valid for the first time step. The problem is similarly solved for the second time step with updated position of the body. Once the new values of the potentials are found, the time derivatives of the potential can be easily estimated for reasonably small time increments.

$$\frac{\partial \phi}{\partial t} = \frac{D\phi}{Dt} - |\nabla \phi|^2 \approx \frac{\Delta \phi}{\Delta t} - |\nabla \phi|^2 \tag{21}$$

If the time derivatives of the flow potentials are estimated, the induced air pressure in the air layer and particularly on the free surface is calculated by using unsteady Bernoulli equation.

$$P = -\rho \left[\frac{\partial \phi}{\partial t} + \frac{1}{2} |\nabla \phi|^2 + g\eta \right] \tag{22}$$

The potential gradients which evaluate the velocity components can be estimated using finite difference method. However, these components can be directly evaluated using following equations to remove all disadvantages of finite difference method.

$$\frac{\partial \phi}{\partial x} = -\int_{\Gamma} \left[\frac{\partial \lambda}{\partial x} \frac{\partial \phi}{\partial n} - \phi \frac{\partial}{\partial x} \left(\frac{\partial \lambda}{\partial n} \right) \right] ds \tag{23}$$

$$\frac{\partial \phi}{\partial y} = -\int_{\Gamma} \left[\frac{\partial \lambda}{\partial y} \frac{\partial \phi}{\partial n} - \phi \frac{\partial}{\partial y} \left(\frac{\partial \lambda}{\partial n} \right) \right] ds \tag{24}$$

Figure 3illustrates typical non-dimensional velocity components using Equations 23 and 24.

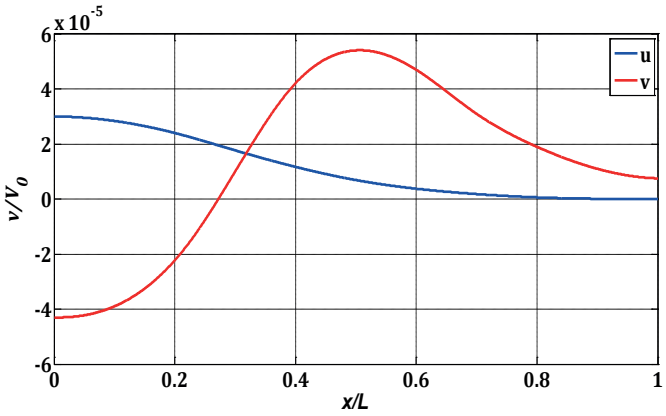

Fig. 3. Typical velocity components on the free surface interface

After the second time step, the induced air pressure on the free surface is known and the numerical solution of the water problem can be started. The primary boundary conditions of the water problem is the symmetry line and the free surface. There is also another boundary condition which closes the domain with far-field boundary condition. This domain is not included in the solution because the BEM is independent of far-field boundary condition in the present problem. From kinetic boundary condition, the induced air pressure in each time step is main source of disturbance in the water problem. Again, the number of known and unknown parameters for the water problem is the same and the system of linear algebraic equations can be solved using different method such as Gauss–Seidel method. The water problem is solved at the current time step of the air problem. Once the water problem is also solve, the free surface profile is updated using velocity component of water problem that estimated from solution of water flow. At the first and second time step, the boundary condition on the free surface is set to free slip condition. In other words, tangential derivatives of the air and water potentials, ϕ_s, are not necessarily the same on the free surface. Therefore, the following kinematic free surface boundary condition readily concluded which must be satisfied on the free surface at each time step.

$$\phi_{na} = \phi_{nw} \tag{25}$$

here the subscripts a and *w*depict the air and water flows, respectively. Moreover, kinetic boundary condition simply relates the air and water pressure at the interface considering the surface tension at two firs time steps.

$$P_w = P_a - \sigma \frac{\partial^2 \eta}{\partial x^2} \tag{26}$$

After updating the free surface profile and the body position, the numerical solution of the problem at the third time step is started and continues. The proposed numerical solution in the present model may called a weakly coupled method between air and water flows. At each time step the pressure on the free surface is evaluated from air problem whereas the free surface profile updated from the water problem. After updating the free surface profile the estimated pressure from the air flow is corrected using parameters water potentials. This corrected pressure field on the interface is used as a boundary condition for the air problem at the next time step.It is worth noting that the all of time derivatives are evaluated using a backward time differencing scheme. So, the time marching is not dependent on the next time step. Therefore, the updated value of potentials can be computed as following.

$$\frac{\partial \phi_w}{\partial t} = -\left(\frac{P_a}{\rho_w} + \frac{1}{2} |\nabla \phi_w|^2 \right) \tag{27}$$

$$\phi_w^{n+1} = \Delta t\left(\frac{\partial \phi_w}{\partial t} + |\nabla \phi_w|^2\right) + \phi_w^n \quad (28)$$

where the superscript n indicates the current time step. The value of time increments for the air problem and the water problem must be the same but not necessarily uniform.

The numerical solution of the problem for the incompressible air flow as well as water problem using boundary element method is fully discussed. The only remaining governing equation is the compressible perturbation Laplace equation. Generally, the numerical procedure is the same. However, special cares should be taken for appropriate transformation of all parameters. Although, the coordinates are transformed into a different computational domain, the discretization and numerical implementation is the same. The solver always check the maximum Mach number of air flow especially at the throat of the gap layer. Once it exceeds 0.3, the solver change the governing equation from an incompressible potential regime to compressible potential flow. To avoid any discontinuity on the obtained results, there is an asymptotic criteria to check the results when the governing equation of the air flow is changed. According to this criteria the time derivative of the pressure on the any arbitrary line such as the interface should be the same at one time step before and after changing of governing equation. Using Taylor expansion these pressure can be stated as follows.

$$P(x, t_s + \Delta t^-)_{y=\eta} = P(x, t_s) + \Delta t^- \frac{\partial P}{\partial t} + O((\Delta t^-)^2) \quad (29)$$

$$P(x, t_s + \Delta t^+)_{y=\eta} = P(x, t_s) + \Delta t^+ \frac{\partial P}{\partial t} + O((\Delta t^+)^2) \quad (30)$$

where Δt^- and Δt^+ are just one time step before and after the time that the governing equation is changed. The time stepwhere numerical method switches from incompressible potential regime to compressible potential regime is indicated by t_s.In other word, the time derivatives of the pressure shoul be the same when $\Delta t \to 0$. If these time derivatives evaluated using backward time differncing the criterai yields:

$$\left[\frac{P(x, t_s) - P(x, t_s + \Delta t^-)}{\Delta t^-} - \frac{P(x, t_s + \Delta t^+) - P(x, t_s)}{\Delta t^+}\right] < \epsilon \quad (31)$$

where ε is a minimum acceptable deviation which is dependent on the problem configuration. If the solver cannot find the solution for satisfying the criteria, it changes the governing equation as the Mach number exceeds 0.3.

The boundary element method is very sensitive to the element size especially when the main source of the disturbance is close to boundaries. At this condition, the element size should be reasonably small enough to resultastable solution. Similar problem also occurs for choosing the proper values of time step. The time increments are determined based on the Courant-Friedrichs-Lowery (CFL) criterion. If the time increment is not selected carefully, the numerical solution suddenly diverges for transformed compressible potential flow.

RESULTS AND DISCUSSIONS:

The present model is developed for large blunt bodies. The main interest is on the common ship sections. Investigation of the air cushioning problem for large ship sections especially during slamming is the main motivation of this study. The common ship sections start from a nearly circular bulbous bow section at the bow to the approximately flat sections at the fore part of the ship. All of these sections are known as blunt sections. To consider all shapes and checking the model response to the body curvature, the geometry of impacting body is first a circle which gradually converts to a flat ellipse as shown in Figure 4. The bluntness of the body is defined as $\zeta = a/b$ and starts from unity for the circle and continues to 10 for a flat ellipse. There are 10 cases corresponding to each integer value of ζ.

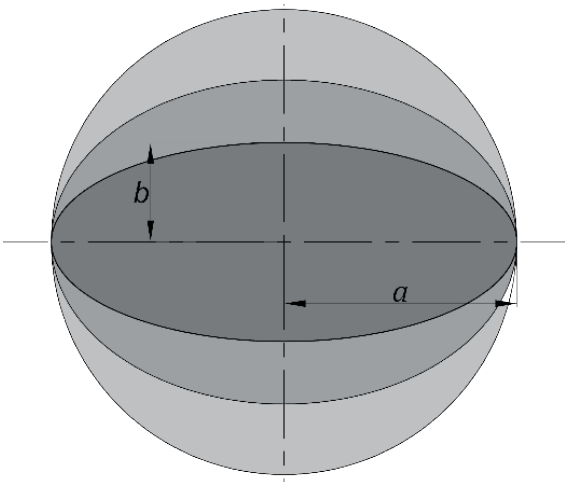

Fig. 4. General representation of the impacting blunt bodies

The numerical simulation starts with a circle and ends with the final flat ellipse. However, only two sets of the results are presented here, for the sake of brevity. The primarily results include the pressure distribution and free surface deformation. Figure 5 depicts pressure distribution for an ellipse with $\zeta = 3$ and and $v_0 = 1$ m/s. The breadth of all sections in the present models is assumed to be the same, $2a = 1$. Additionally, the horizontal direction is presented in non-dimensional form by dividing on the horizontal length scale. Corresponding free surface deformation is also illustrated in Figure 6.

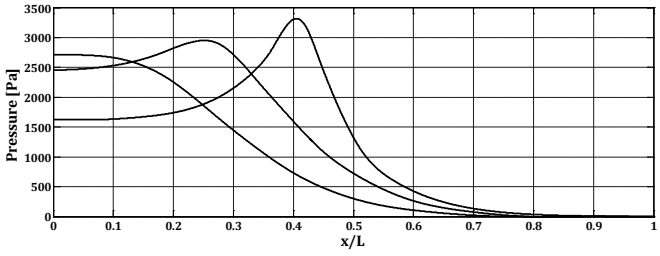

Fig. 5. Pressure distribution for an ellipse with $\zeta = 3$ and $v_0 = 1$ m/s at three consecutive time steps with $\Delta t = 0.008$ ms.

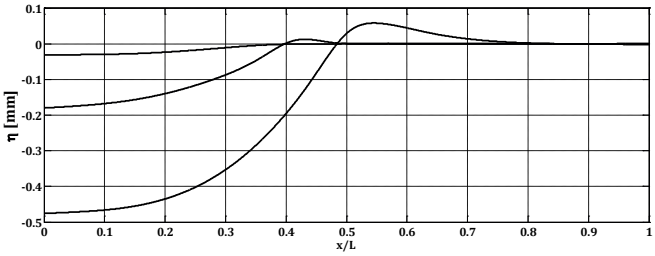

Fig. 6. Free surface deformation for an ellipse with ζ = 3 and v_0=1 m/s at three consecutive time steps with Δt = 0.008 ms.

The maximum pressure at the first time step occurs at origin and exactly beneath the symmetry line of the body. However, the location of the maximum pressure moves toward the throat of the gap layer at the next time step and the keel line pressure reduces. The air pressure rapidly drops after the throat of the layer. As the body gets closer to the free surface, the free surface is more deformed. Since the free surface is deformed, the body will touch the free surface at least on two points. If one can continue the numerical simulation while the body touches the free surface, some amount of air is entrapped between the body and free surface. Similar simulation can be also carried out for a blunter body. Figure 7 illustrates the maximum pressure distribution for an ellipse with ζ = 7 and v_0 = 1. The main difference between this new evaluated pressure and the previous one for ζ = 3, is the behavior of the air pressure. The solver predicts an impulsive response for the induced pressure. The maximum peak pressure also dramatically increases due to contribution of longer part of the body in comparison with the previous body. Although the predicted pressure corresponds with the air flow, its magnitude is in the same order of hydrodynamic impact pressure.

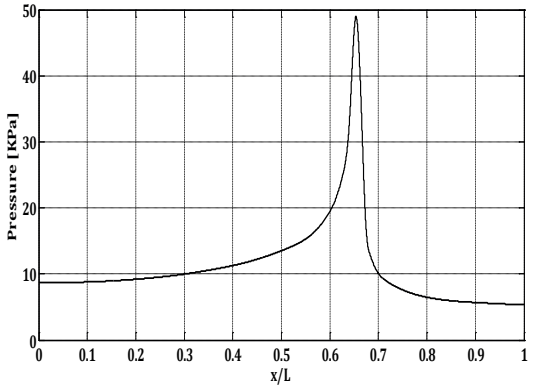

Fig. 7. Pressure distribution for an ellipse with ζ = 7 and v_0 = 1 m/s.

The evaluated pressure distribution for the blunter body shows a keel pressure three times more that the peak pressure of the previous body. In fact, the air layer can effectively tolerate a high pressure. This can significantly reduce the impact speed. One may further develop the present model to consider a rigid body dynamic equation to estimate the speed reduction. Theinduced high pressure compresses the air flow. Consequently, the governing equation should be changed to a compressible flow. To investigate this case, maximum air velocity for both bodies are evaluated and shown in Figure 8.

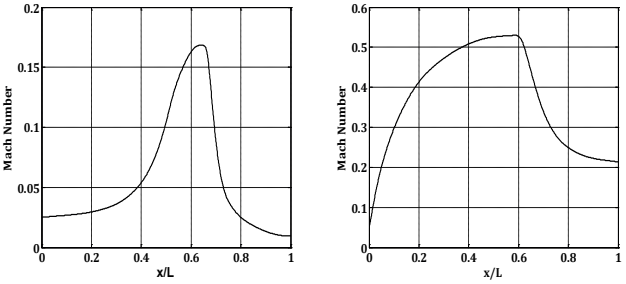

(a) *(b)*

*Fig. 8. Maximum air velocity for (**a**) An ellipse with ζ = 3 and (**b**) An ellipse with ζ = 7.*

For both bodies the maximum velocity occurs at the throat of the air gap layer. However, the behavior is completely different. It is clearly shown that the bluntness of the body can change the induced air speed. The maximum speed in the blunter body exceeds 0.3 and the flow is certainly compressible. The evaluated velocity speed shows that from x/L = 0.1, the Mach number is about 0.3.Additionally, the velocity of air flow after the throat is still considerably high. This can be also interpreted from the impulsive pressure reported in Figure 7. This suggests that another air cushioning layer may form after the throat but with much smaller length scales.

The accuracy of all numerical methods is dependent on the element size. Therefore, a mesh independency analysis should be always carried out to assess the whole performance of the numerical method. Boundary element method is also very sensitive to the element size especially close to the sources of disturbances. Figure 9 indicates mesh dependency analysis which typically figured out for an ellipse with ζ = 4. The error is defined based on the maximum pressure. Similar analysis is also conducted for all other cases.

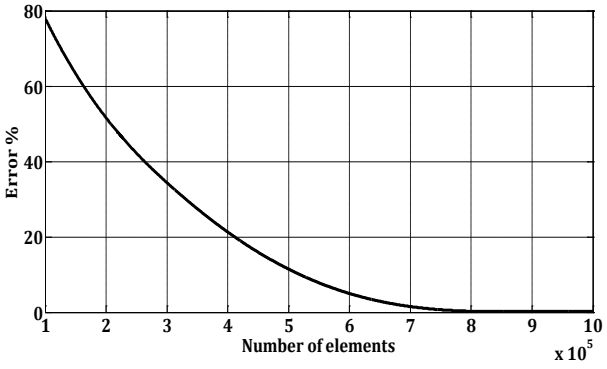

Fig. 9. Mesh dependency analysis

The cushioning problem is a complicated problem and all published researches focus on the special aspects of the problem with different assumption and limitation. This makes it difficult to find a general problem which can be used as a bench mark for long range of applications. Unfortunately,

the most of study considers the cushioning problem for small scale impacting bodies such as droplet impacts. However, there are studies which may be considered for validation such as those carried out by Hicks and Purvis [5, 6 and 7] and Hicks et al. [8]. The assumptions and the geometries are not the same as those considered in the present model but their model is effectively available for large sections. The Hicks and Purvis method has been used and a computer code developed to calculate cushioning problem for large blunt bodies. Figure 10 shows the comparison of the results of the present method with Hicks and Purvis method for two ellipses with ζ = 3 and ζ = 7.

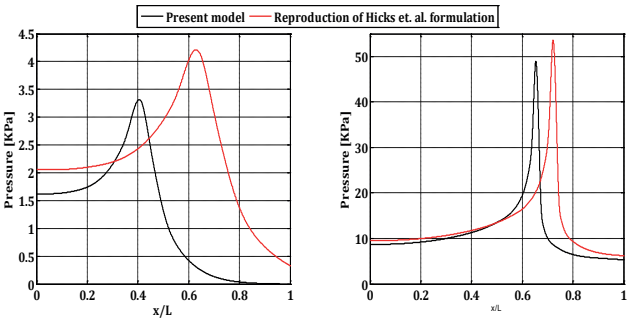

*Fig. 10. Evaluation of the present method and Hicks and Purvis method. **(a)** for a 2D ellipse with and **(b)** for a 2D ellipse with ζ = 7. The Hicks and Purvis results are reproduced by the Authors for the corresponding geometries.*

The comparison depicts that the tendency of the both methods are the same. The blunter body shows a better agreement between both methods. The main source of deviation is neglecting lubrication region in the present method. It can be shown that considering such a region may result in a higher cushioning pressure. However, Mandre and Brenner [9] showed that the high pressure may not happen in real practice where the cushioning layer collapses before experience very high pressure. Anyhow, motivation of this method is to use a simple method by disregarding lubrication layer effect. The method is applicable for the very blunt and large bodies.

CONCLUSIONS

Numerical simulation of the air cushioning problem is investigated in this study. The proposed method based on two different governing equations for modeling the air flow including the incompressible and compressible flow which both are potential. The governing equations are in the forms of Laplace equation. The equation is solved using an iterative boundary element method. Pressure distribution and free surface profile are estimated for different blunt bodies. Typical results corresponding to two ellipses with ζ = 3 and ζ = 7 are presented. It is shown that as the bluntness of the body increases the induced pressure increases and the resulting water surface profile rises. Comparison of the present method with analytical method of Hicks and Purvis shows that the inviscid potential method can fairly approximate the problem for very blunt bodies. Additionally, the behavior of the air pressure for the blunter body is impulsive and the magnitude of the peak pressure is in order of impact pressure of water entry. This suggests that the cushioning problem cannot be neglected for very blunt bodies in water entry problem.

LIST OF SYMBOLS

Below is the list of symbols which are employed in the present text.

ρ_a	Air density
ρ_w	Water density
σ	Air-Water surface tension
P	Pressure
ϕ	Velocity potential
λ	Fundamental solution of Laplace equation
η	Free surface profile
κ	Curvature
$\hat{n}$	Norma vector
H_{ij}, G_{ij}	Influence coefficients
g	Gravitational acceleration
ds	Length differential
Γ	Boundary identity
a, b	Dimensions of an ellipse
ζ	Ellipse dimensional ratio

REFERENCES

1. J.H.G., Verhagen, 1967,"The impact of a flat plate on a water surface.", J. Ship research 11, 211-233.

2. O. Reynolds, 1886, "On the theory of lubrication and its application to Mr. Beauchamp tower's experiments, including an experimental determination of viscosity of olive oil." Philos. Trans. R. Soc. London Ser. A 177, 157-234.

3. N.G., Asryan, 1972, "Solid plate impact on surface of incompressible fluid in the presence of a gas layer between them.", SSR Mek25, 32{49.

4. S.K., Wilson, 1991, "A mathematical model for the initial stages of fluid impact in the presence of a cushioning fluid layer.", J. Engineering mathematics 25, 265-285.

5. P. Hicks and R. Purvis, 2010, "Air cushioning and bubble entrapment in three-dimensional droplet impacts." J. Fluid Mechanics 649, 135-163.

6. P. Hicks and R. Purvis, 2011, "Air cushioning in droplet impacts with liquid layers and other droplets." Physics of fluids 23.

7. P.D. Hicks and R. Purvis, 2013, "Liquid solid impacts with compressible gas cushioning." Journal of Fluid Mechanics 735, 120-149.

8. P.D. Hicks, E.V. Ermanyuk, N.V. Gavrilov, and R. Purvis, 2012, "Air trapping at impact of a rigid sphere onto a liquid." J. Fluid Mechanics 695, 310-320.

9. S. Mandre and M.P. Brenner, 2012, "The mechanism of a splash on a dry solid surface." Journal of Fluid Mechanics 690, 148-172.

10. F.T. Smith, L.Li and G.X. Wu, 2003,"Air cushioning with a lubrication/inviscid balance." Journal of Fluid Mechanics 482, 291-318

11. J.O. Marston, I.U. Vakarelski, and S.T. Thoroddsen, 2011, "Bubble entrapment during sphere impact onto quiescent liquid surfaces." J. Fluid Mechanics 680, 660-670

12. T. Tran, H. de Maleprade, C. Sun, and D. Lohse, 2013, "Air entrainment during impact of droplets on liquid surfaces." J. Fluid Mechanics 726.

13. G.R.G. Lewison, and W.M. Maclean, 1968, "On the cushioning of water impact by entrapped air." J. Ship research 12, 116-130

14. S.T. Thoroddsen, T.G. Etoh, K. Takehara, N. Ootsuka and Y. Hatsuki, 2005 "The air bubble entrapped under a drop impacting on a solid surface." J. Fluid Mechanics 545, 203-212.

15. W. Bouwhuis, M.H.W. Hendrix, M.H.W., D. van der Meer, and J.H. Snoeijer, 2015, "Initial surface deformations during impact on a liquid pool." J. Fluid Mechanics 771, 503-519.

16. J.T. Katsikadelis, "BOUNDARY ELEMENTS: Theory and Applications", Elsevier, 2002

CONTACT WITH THE AUTHORS

MojtabaBarjasteh

Hamid Zeraatgar
e-mail: hamidz@aut.ac.ir

Amirkabir Laboratory of Hydrodynamics (ALH)
Faculty of Maritime Engineering
Amirkabir University of Technology
Tehran
Iran